

 Open access • Posted Content • DOI:10.1101/2020.07.17.20152702

Evaluation of efficiency and sensitivity of 1D and 2D sample pooling strategies for diagnostic screening purposes — [Source link](#)

Jasper Verwilt, Pieter Mestdagh, Jo Vandesompele

Institutions: Ghent University

Published on: 17 Aug 2020 - medRxiv (Cold Spring Harbor Laboratory Press)

Topics: Pooling and Sample (statistics)

Related papers:

- [Optimizing digitalization effort in morphometrics.](#)
- [Approximate Quality Assessment with Sampling Approaches](#)
- [Cost-effective regression testing through Adaptive Test Prioritization strategies](#)
- [Predicting the cost-effectiveness of regression testing strategies](#)
- [Practical Outcomes of Applying Ensemble Machine Learning Classifiers to High-Throughput Screening \(HTS\) Data Analysis and Screening](#)

Share this paper:    

View more about this paper here: <https://typeset.io/papers/evaluation-of-efficiency-and-sensitivity-of-1d-and-2d-sample-4bg30fxd48>

1 **Evaluation of efficiency and sensitivity of 1D and 2D sample**
2 **pooling strategies for SARS-CoV-2 RT-qPCR screening purposes**

3 Running title: *Evaluation of SARS-CoV-2 RT-qPCR pooling*

4 **Jasper Verwilt^{1,2,3}, Jan Hellemans⁴, Tom Sante^{2,3}, Pieter Mestdagh^{1,2,3,4}, Jo**

5 **Vandesompele^{1,2,3,4}**

6 *1 OncoRNALab, Cancer Research Institute Ghent, Corneel Heymanslaan 10, 9000*

7 *Ghent, Belgium*

8 *2 Department of Biomolecular Medicine, Ghent University, Corneel Heymanslaan 10,*

9 *9000 Ghent, Belgium*

10 *3 Center for Medical Genetics, Ghent University, Corneel Heymanslaan 10, 9000*

11 *Ghent, Belgium*

12 *4 Biogazelle, Technologiepark 82, 9052 Zwijnaarde, Belgium*

13
14 • 17 text pages

15 • 4 figures

16
17 Corr. author:

18 Jo Vandesompele

19 Corneel Heymanslaan 10, 9000 Gent, Belgium

20 +32 9 332 55 32

21 jo.vandesompele@ugent.be

22
23 Funding: UGent BOF-GOA LNCCA (BOF16/GOA/023, J.Va.)

24

25 **Abstract**

26 To increase the throughput, lower the cost, and save scarce test reagents,
27 laboratories can pool patient samples before SARS-CoV-2 RT-qPCR testing. While
28 different sample pooling methods have been proposed and effectively implemented
29 in some laboratories, no systematic and large-scale evaluations exist using real-life
30 quantitative data gathered throughout the different epidemiological stages. Here, we
31 use anonymous data from 9673 positive cases to simulate and compare 1D and 2D
32 pooling strategies. We show that the optimal choice of pooling method and pool size
33 is an intricate decision with a testing population-dependent efficiency-sensitivity
34 trade-off and present an online tool to provide the reader with custom real-time
35 pooling strategy recommendations.

36 Introduction

37 One of the key strategies in the global battle against the COVID-19 pandemic is
38 massive population testing. However, an ongoing shortage of time, reagents and
39 testing capacity has tempered these efforts. Pooled testing of samples presents itself
40 as a valid strategy to overcome these hurdles and to realize rapid, large-scale testing
41 at lower cost and lower dependence on test reagents.

42

43 Multiple recent studies discussed pooling strategies in the frame of SARS-CoV-2
44 testing. Researchers have explored many strategies, but two of them have been
45 welcomed for their simplicity and effectiveness: one-time pooling (1D pooling) and
46 two-dimensional pooling (2D pooling). In 1D pooling, the samples are pooled, pools
47 are tested and samples in positive pools are tested individually (Figure 1)¹⁻⁴. Labs
48 worldwide have extensively evaluated 1D pooling strategies for SARS-CoV-2 testing
49 in the lab⁵⁻⁸ or using simulations¹. In 2D pooling, samples are organized in a 2D
50 matrix and pools are created along the matrix's rows and columns. The pools are
51 tested, and negative rows and columns are excluded from the matrix. Next, all
52 remaining samples are tested individually (Figure 1)⁹. Other more complex strategies
53 exist, such as repeated pooling¹, P-BEST¹⁰ and Tapestry¹¹.

54

55 While attractive, pooling strategies come with inherent limitations. First, pooling
56 dilutes each sample, possibly to such an extent that the viral RNA becomes
57 undetectable, which results in false negative observations^{8,9,12}. A second limitation is
58 that an increase in sample manipulations augments the risk of cross-contamination
59 and sample mix-ups, possibly leading to false negatives and false positives⁹. Last,
60 when pooling, identifying individual positive samples will take an additional RNA

61 extraction and RT-qPCR run, while one run is sufficient when testing individual
62 samples without pooling.

63

64 Although the number of preprints and peer-reviewed publications on pooling
65 strategies for COVID-19 RT-qPCR-based testing has accelerated rapidly throughout
66 the pandemic, some critical aspects remain mostly ignored. First of all, the proposed
67 optimal pooling strategy is most often based on a binary classification of samples as
68 either positive or negative. This Boolean approach is not true to the real-world
69 situation and does not investigate the pooling step's dilution effect. Second, when
70 using Cq values as a semi-quantitative measure¹³ of the viral loads, their overall
71 distribution should reflect the real-life population. A high fraction of Cq values close to
72 the limit of detection of the RT-qPCR assay produces an elevated risk of resulting in
73 false negative samples¹⁴. Last, since the Cq distribution of the sample population and
74 prevalence may vary over time, it remains unclear how the pooling strategy's
75 performance evolves as the pandemic progresses.

76

77 We questioned to what extent optimal pooling strategies would have changed
78 throughout the COVID-19 pandemic and how testing facilities might use pooling
79 strategies for future testing in a correct and attainable manner. To this extent, we
80 simulated and evaluated one-dimensional (1D) and two-dimensional (2D) pooling
81 strategies with different pool sizes using real-life RT-qPCR data gathered by the
82 Belgian national testing platform during the end of the first and the beginning of the
83 second SARS-CoV-2 epidemiological waves. Additionally, we formulate a detailed
84 action plan to provide testing laboratories with the most suitable pooling strategy
85 assuring an optimal efficiency-sensitivity trade-off.

86

87 **Materials and Methods**

88 *Patient samples*

89 Nasopharyngeal swabs were taken by a healthcare professional as a diagnostic test
90 for SARS-CoV-2, as part of the Belgian national testing platform. The individuals
91 were tested at nursing homes or in triage centers, between April 9th and June 7th, and
92 between September 1st and November 10th. After filtering the data as described
93 further, this resulted in 207 944 patients in total, of which 9673 positives (4.65%).

94

95 *SARS-CoV-2 RT-qPCR test*

96 During the first (spring) wave, RNA extraction was performed using the Total RNA
97 Purification Kit (Norgen Biotek #24300) according to the manufacturer's instructions
98 using 200 µl transport medium, 200 µl lysis buffer and 200 µl ethanol, with
99 processing using a centrifuge (5810R with rotor A-4-81, both from Eppendorf). RNA
100 was eluted from the plates using 50 µl elution buffer (nuclease-free water), resulting
101 in approximately 45 µl eluate. RNA extractions were simultaneously performed for 94
102 patient samples and 2 negative controls (nuclease-free water). After addition of the
103 lysis buffer, 4 µl of a proprietary 700 nucleotides spike-in control RNA (prior to May
104 25th, 40 000 copies for singleplex RT-qPCR; from May 25th onwards, 5000 copies for
105 duplex RT-qPCR) and carrier RNA (200 ng of yeast tRNA, Roche #10109517001)
106 was added to all 96 wells from the plate. To the eluate of one of the negative control
107 wells, 7500 RNA copies of positive control RNA (Synthetic SARS-CoV-2 RNA
108 Control 2, Twist Biosciences #102024) were added. During the second (autumn)
109 wave, RNA extraction was performed using the Quick-RNA Viral 96 Kit (Zymo
110 Research #R1041), according to the manufacturer's instructions using 100 µl

111 transport medium, with processing using a centrifuge (5810R with rotor A-4-81, both
112 from Eppendorf). RNA was eluted from the plates using 30 µl elution buffer
113 (nuclease-free water). RNA extractions were simultaneously performed for 92 patient
114 samples, 2 negative controls (nuclease-free water), and 2 positive controls (1 diluted
115 positive case as a full workflow control; 1 positive control RNA as RT-qPCR control,
116 see further). After addition of the lysis buffer, 4 µl of a proprietary 700 nucleotides
117 spike-in control RNA (5000 copies) and carrier RNA (200 ng of yeast tRNA, Roche
118 #10109517001) was added to all 96 wells from the plate. To the eluate of one of the
119 negative control wells, 7500 RNA copies of positive control RNA (Synthetic SARS-
120 CoV-2 RNA Control 2, Twist Biosciences #102024) were added.

121 Six µl of RNA eluate was used as input for a 20 µl RT-qPCR reaction in a CFX384
122 qPCR instrument using 10 µl iTaq one-step RT-qPCR mastermix (Bio-Rad
123 #1725141) according to the manufacturer's instructions, using 250 nM final
124 concentration of primers and 400 nM of hydrolysis probe. Primers and probes were
125 synthesized by Integrated DNA Technologies using clean-room GMP production. For
126 detection of the SARS-CoV-2 virus, the Charité E gene assay was used (FAM)¹⁵; for
127 the internal control, a proprietary hydrolysis probe assay (HEX) was used. Prior to
128 May 25th, 2 singleplex assays were performed; from May 25th onwards, 1 duplex RT-
129 qPCR was performed. Cq values were generated using the FastFinder software
130 v3.300.5 (UgenTec). Only batches were approved with a clean negative control and
131 a positive control in the expected range.

132

133 *Digital PCR calibration of positive control RNA*

134 Digital PCR was done on a QX200 instrument (Bio-Rad) using the One-Step RT-
135 ddPCR Advanced Kit for Probes (Bio-Rad #1864022) according to the

136 manufacturer's instructions. Briefly, 22 μ l pre-reactions were prepared consisting of 5
137 μ l 4x supermix, 2 μ l reverse transcriptase, 6 μ l positive control RNA (125 RNA
138 copies/ μ l), 15 mM dithiothreitol, 900 nM of each forward and reverse primer and 250
139 nM *E* gene hydrolysis probe (FAM) (see higher). 20 μ l of the pre-reaction was used
140 for droplet generation using the QX200 Droplet Generator, followed by careful
141 transfer to a 96-well PCR plate for thermocycling: 60 min 46 °C reverse transcription,
142 10 min 95 °C enzyme activation, 40 cycles of 30 sec denaturation at 95 °C and 1 min
143 annealing/extension at 59 °C, and finally 10 min 98 °C enzyme deactivation. Droplets
144 were analyzed by the QX200 Droplet Reader and QuantaSoft software. With an RNA
145 input of 7500 copies per reaction, the digital PCR result was 1500 cDNA copies (or
146 20% of the expected number, a fraction confirmed by Dr. Jim Huggett for particular
147 lot numbers of #102024, personal communication). The median Cq value of the
148 positive control RNA of 24.55 thus corresponds to 1500 digital PCR calibrated cDNA
149 molecules.

150

151 *Determination of efficiency and sensitivity for simulated of 1D and 2D pooling*
152 *strategies*

153 Simulations are run using R 4.0.1. First, several cohorts of 100 000 patients are
154 repeatedly simulated with varying fractions of positive cases f , depending on the
155 fraction of positive samples of the investigated week. This is done five times,
156 resulting in five replicate cohorts per week. The Cq values of the positive samples
157 are sampled with replacement from the set of the positive Cq values of said week.
158 Next, the patients are randomly separated into pools depending on the pooling
159 strategy that is simulated. The pooling strategies that were simulated are 1x4, 1x8,

160 1x12, 1x16, 1x24 (all 1D), and 8x12, 12x16 and 16x24. The Cq value of the pool was
161 calculated as follows:

162

$$c_{pool} = \log_2 P - \log_2 \sum_{i=1}^p 2^{-c_i} \quad \#(1)$$

163

164

165 With c_{pool} the Cq value of the pool, P the number of samples in the pool, p the
166 number of positive samples in the pool, c_1, c_2, \dots, c_p the Cq values of the positive
167 samples. If the Cq value of the pool is lower than the single-molecule Cq value, it is
168 classified as a positive pool. For 1D pooling, only samples in positive pools are
169 retained and the remaining individual Cq values were checked to be positive. For 2D
170 pooling, the Cq values of the differently sized pools are checked simultaneously and
171 the samples in negative pools are removed, after which all Cq values of the
172 remaining samples are checked individually. Samples that were retained after the
173 testing of the pools and that had an individual Cq lower than the single-molecule Cq
174 value are classified as positive, all other samples are classified as negative.

175 The sensitivity is calculated as:

176

$$sensitivity = \frac{no. \text{ true positive samples}}{no. \text{ true positive samples} + no. \text{ false negative samples}} \quad \#(2)$$

177

178

179 The analytical efficiency gain is calculated as:

180

$$efficiency\ gain = \frac{no.\ tests\ required\ for\ individual\ testing}{no.\ tests\ required\ for\ pooling\ strategy} \#(3)$$

181

182

183 In all simulations, the number of tests required for individual testing is equal to the

184 number of samples (assuming no technical failures). The outcomes for each

185 simulation were identical as the sample size far outreached the size of the dataset.

186 The code is available at <https://github.com/OncoRNALab/covidpooling>.

187

188 *Ad hoc sensitivity and efficiency calculation*

189 To calculate the efficiency for a specific 1D pooling strategy on a real sample set, the

190 following equation was used:

$$efficiency = \frac{n}{\frac{n}{s} \cdot (1 + s \cdot \sum_{k=1}^s \left(\frac{s!}{k!(s-k)!} \cdot p^k \cdot (1-p)^{s-k} \cdot (1-c^k) \right))} \#(4)$$

191

192 With sample size n , pool size s , fraction of positive samples p and fraction of Cq

193 values of positive samples above the 'dilution detection limit': the lowest individual Cq

194 value that can result in a pooled Cq value lower than the single molecule Cq value,

195 or:

$$single\ molecule\ Cq\ value - \log_2(pool\ size) \#(5)$$

196

197 Equation (4) is derived as follows. The efficiency is defined by the following equation:

$$efficiency = \frac{n}{no.\ tests\ required\ for\ pooling\ strategy} \#(6)$$

198

199 The number of tests performed when using a pooling strategy is equal to:

$$no.\ tests\ required\ for\ pooling\ strategy = no.\ pools + no.\ positive\ pools \cdot s \#(7)$$

200

201 Since # pools = $\frac{n}{s}$,

$$\text{no. tests required for pooling strategy} = \frac{n}{s} + \text{no. positive pools} \cdot s \#(8)$$

202 The exact number of positive pools can be calculated by multiplying the number of
203 pools by the probability of a pool testing positive. Approximately, a pool will test
204 positive if it includes a positive sample with a Cq value lower than the 'dilution
205 detection limit'. The probability of having a specific number of positive samples k in a
206 pool with pool size s is defined by a binomial distribution:

$$\frac{s!}{k!(s-k)!} \cdot p^k \cdot (1-p)^{s-k} \#(8)$$

207

208 Thus, the probability of having at least one positive value in a pool is equal to:

$$\sum_{k=1}^s \left(\frac{s!}{k!(s-k)!} \cdot p^k \cdot (1-p)^{s-k} \right) \#(10)$$

209

210 In general, we can assume that when a sample has a Cq value higher than the
211 'dilution detection limit', for the sample to test positive, it must be accompanied by a
212 sample with a Cq value lower than the 'dilution detection limit'. Equation (10) can be
213 adjusted to factor for these events:

$$\sum_{k=1}^s \left(\frac{s!}{k!(s-k)!} \cdot p^k \cdot (1-p)^{s-k} \cdot (1-c^k) \right) \#(10)$$

214

215 Filling in Eq. (10) in Eq. (8) results in the final formula being used for the calculation
216 of the efficiency.

217

218 To estimate the sensitivity for a specific 1D pooling strategy on a real sample set, the
219 following equation was used:

$$sensitivity = c \cdot \sum_{k=0}^{s-1} \left(\frac{(s-1)!}{k! ((s-1)-k)!} \cdot p^k \cdot (1-p)^{(s-1)-k} \cdot (1-c^k) \right) + (1-c) \quad \#(11)$$

220

221 The sensitivity can be defined as the probability a true positive sample tests positive.

222 For our situation it will be equal to the probability that any sample tests positive:

$$P(pos\ test) = P(pos\ test|Cq \geq\ cut\ off) \cdot P(Cq \geq\ cut\ off) + P(pos\ test|Cq <\ cut\ off) \cdot P(Cq <\ cut\ off) \quad \#(12)$$

223

224 Previously, $P(Cq \geq\ cut\ off)$ was defined as c and therefore $P(Cq <\ cut\ off) = 1 - c$.

225 Also $P(pos\ test|Cq <\ cut\ off) = 1$. A positive sample with Cq value above the

226 'dilution detection limit' can only test positive if one of the other samples in the pool is

227 also positive and has a Cq value lower than the 'dilution detection limit'. We can

228 calculate the probability of this happening by using the same logic as before, but with

229 $s - 1$ instead of s :

$$\sum_{k=0}^{s-1} \left(\frac{(s-1)!}{k! ((s-1)-k)!} \cdot p^k \cdot (1-p)^{(s-1)-k} \cdot (1-c^k) \right) \quad \#(13)$$

230

231 Completing Eq. (12) with Eq. (13) leads to Eq. (11) for calculating the sensitivity.

232

233 *Shiny application*

234 To help laboratories find the best pooling strategy for their specific situation (i.e. the

235 local positivity ratio and Cq value distribution), we developed a Shiny application in R

236 4.0.1. The Shiny application was launched on our in-house Shiny server and is

237 available at <https://shiny.dev.cmgg.be/>.

238

239

240 **Results**

241 *Single-molecule Cq value determination*

242 We made a 5-point 10-fold serial dilution series of positive control RNA from 150 000
243 (digital PCR calibrated) copies down to 15 copies. The Y-intercept value points at a
244 single-molecule Cq value of 35.66 and 35.28 for singleplex and duplex RT-qPCR,
245 respectively (Supplemental Figure 1). Therefore, we conservatively use 37 as the
246 single-molecule value for further analysis. Patient sample Cq values higher than the
247 single-molecule Cq value threshold are likely due to random measurement variation,
248 lot reagent variability and sample inhibition.

249

250 *Cq distribution is dynamic over course of the pandemic*

251 Few studies have explored how the Cq value distribution within one testing facility
252 evolves during the COVID-19 pandemic. We determined the 75%-tile of the Cq value
253 distribution and the percentage of positive tests per day as a proxy for actual Cq
254 value distribution and prevalence, respectively (Figure 2). We compared the fraction
255 of positive tests in our dataset with the fraction of positive tests as reported by the
256 federal agency for public health Sciensano (<https://epistat.wiv-isp.be/covid/>.
257 accessed January 25th, 2021). First, the fractions of positive tests seem to align at
258 the end of the first wave, but in the second wave our data seems to be shifted about
259 one to two weeks later. Second, the 75%-tile of the Cq values varies over the course
260 of the pandemic from a minimum value of around 18 and a maximum value of almost
261 35. Third, when comparing the fraction of positive samples and the 75%-tile of the Cq
262 value distribution, we note that these parameters are inversely related: when the

263 positivity rate goes down, the Cq value distribution shifts towards the higher end of
264 the spectrum. In conclusion, the Cq value distribution and prevalence show a
265 dynamic profile over the course of the COVID-19 pandemic. These observations are
266 crucial considering that positivity rate and Cq value distribution are key determinants
267 of efficiency and sensitivity of any pooling strategy.

268

269 *Pooling efficiency and sensitivity changes as pandemic progresses*

270 To explore how hypothetical pooling strategies would have affected the SARS-CoV-2
271 testing outcomes, we simulated different 1D (with pool size of 4, 8, 12, 16 and 24)
272 and 2D pooling (with pool sizes of 8x12, 12x16, and 16x24) strategies using
273 individual sample Cq values from a single Belgian laboratory during the end of the
274 first and beginning of the second wave. The data was grouped by week and the
275 resulting Cq value distributions and positivity rates were used as input for the
276 simulations (Figure 3). First, sensitivity and efficiency show very opposing patterns
277 when comparing different timeframes during the pandemic. At the end of the first
278 wave the efficiency increases, while at the beginning of the second wave, the
279 efficiency decreases. The sensitivity drops as we move further away from the first
280 wave but remains stable as we enter the second. Second, pool size and strategy
281 have a major influence on the outcomes. 2D pooling strategies generally have the
282 highest efficiency, but the lowest sensitivity. Curiously, strategies with larger pool
283 sizes were more efficient during the end of the first wave, but less efficient during the
284 beginning of the second wave. The sensitivity was always higher for strategies with
285 smaller pool sizes, irrespective of the time during the pandemic. We conclude that—
286 just like the positivity rate and the Cq value distribution—the sensitivity and efficiency

287 depend on the timing in the pandemic and are heavily affected by the pooling
288 strategy and the size of the pools.

289

290 *Positivity rate drives efficiency, Cq distribution drives sensitivity*

291 We wondered how the positivity rate, Cq value distribution and pooling strategy affect
292 the performance of the adopted strategy. To investigate this, we used the previous
293 simulations for the end of the first wave to create an adjusted visualization where all
294 parameters involved are incorporated (Figure 4). First, it is apparent that weeks with
295 a high 75%-tile Cq value tend to have a low sensitivity and weeks with a high
296 positivity rate seem to have a low efficiency. Second, pooling strategies with smaller
297 pool sizes seem less sensitive to changes in positivity rate and Cq value distribution,
298 as indicated by the area of the polygon traced around the edges of the data (Figure
299 4). These results show that the prevalence mainly contributes to the efficiency and
300 the Cq distribution to the sensitivity.

301

302 *Shiny app for guided decision making*

303 To provide laboratories with a custom pooling strategy recommendation based on
304 their specific sampling population, we worked out equations to estimate the
305 sensitivity and efficiency (for 1D pooling strategies) based on an uploaded dataset of
306 Cq values. The derivation of these equations can be found in the Methods section.
307 We focused on 1D pooling strategies since 2D pooling strategies generally resulted
308 in extreme outcomes (highest efficiency and lowest sensitivity) and the outcomes of
309 the optimal pooling strategy are situated somewhere in two extremes. To evaluate
310 the equations' capacities to replicate the simulations, we compared the simulated
311 efficiency and sensitivity of the pooling strategies for the different weeks and the

312 efficiency and sensitivity of the pooling strategies the distributions, fraction of positive
313 samples and single-molecule cutoff as inputs for the formulas (Supplemental Figure
314 2 and Supplemental Figure 3). We integrated these formulas into an open-access
315 Shiny application (Supplemental Figure 4). The application requires three inputs: a
316 dataset of Cq values from positive samples, the positivity rate and the single-
317 molecule cut-off Cq value. The Shiny application will then swiftly output the estimated
318 data-specific efficiency and sensitivity for different pooling strategies.

319

320 **Discussion**

321 Using a sizeable real-life dataset of 9673 SARS-CoV-2 positive nasopharyngeal
322 samples, we found that the pooling strategies' sensitivity and efficiency mainly
323 depend on the prevalence and the distribution of the Cq values. Our results indicate
324 that both the prevalence and the Cq value distribution are dynamic parameters
325 during the SARS-CoV-2 pandemic and that, as a result, the resulting sensitivity and
326 efficiency of pooling strategies are as well. To enable researchers and institutions
327 with a real-time and accessible recommendation concerning the optimal 1D pooling
328 strategy for their testing population, we developed a Shiny app providing just that.

329 Two factors could explain the dynamics of the prevalence and the Cq value
330 distribution: epidemiological and virological change within the same sampling
331 population and variation in the sampling population. The existence of these factors
332 would suggest that an intricate interplay of these two components is at the origin of
333 the observed evolutions. Recent research indicated that the first component
334 (epidemiological change) exists, as the distribution of random surveillance testing-
335 deduced Cq values fluctuates during the SARS-CoV-2 pandemic (by definition, no
336 changes in sampling population occurred in this research, thereby excluding this

337 factor from the equation)¹⁶. The second component (variation in sampling population)
338 is bound to happen when the testing facility is not consistently receiving samples
339 from the same origin, as is the case for Biogazelle. At the very introduction of
340 Biogazelle as a testing facility, most samples originated from hospitals and sources
341 were added progressively as the testing capacity increased. Additionally, the Belgian
342 government instituted a rapid change in the testing regime on October 21st, 2020:
343 only symptomatic suspected SARS-CoV-2 cases get tested. The federal government
344 lifted this measure on November 23rd, 2020, when the number of cases lowered and
345 the existing testing capacity sufficed again. Since symptomatic patients generally
346 show lower Cq values^{17,18}, it is clear that sampling bias will contribute to the overall
347 Cq value distribution.

348 The influence these dynamic parameters have on the variation of performance of
349 pooling strategies is significant. This observation raises an issue for interpreting
350 pooling strategy evaluations not based on time-series datasets. The effectiveness of
351 a chosen pooling plan might even decrease to such an extent that it becomes inferior
352 to individual testing. We observed this situation at the end of the second wave when
353 efficiency is close to 1, but sensitivity is not (Figure 3). Based on these results, it
354 becomes essential to regularly re-evaluate an adopted pooling strategy to avoid
355 compromising on sensitivity and efficiency when there is no need.

356 Multiple effects contribute to how the testing population's characteristics drive pooling
357 strategy outcomes. The main trends show that the prevalence mainly influences
358 efficiency, and the Cq value distribution mainly influences sensitivity (Figure 3). We
359 can explain both observations by using common sense and basic mathematics.
360 When the prevalence is low, the efficiency is high: fewer pools will have positive
361 samples and therefore test negative, which will automatically result in a lower number

362 of tests needed to test all samples. Additionally, when a considerable proportion of
363 samples have a Cq value close to the single-molecule Cq value, a more significant
364 fraction of samples will become too diluted to detect during pooling and result in false
365 negatives. There appear to be secondary compensating effects of the Cq value
366 distribution and prevalence on the efficiency and sensitivity, respectively, which are
367 more subtle. Primarily, as a higher fraction of positive samples has a Cq value close
368 to the upper limit, more pools will test (false) negative, boosting the efficiency. On the
369 other hand, when the prevalence increases, the sensitivity will increase due to an
370 effect we call 'rescuing': a high Cq value that would otherwise test negative when
371 diluted in the pool is 'rescued' by a low Cq value in the same pool. When the
372 prevalence rises, the chances of this phenomenon happening also increase and as
373 will the sensitivity. The same was observed by Cleary et al.¹⁹. Although minor, these
374 secondary effects explain a number of our observations.

375 To elaborate how the optimal pooling strategy (best efficiency trade-off) transforms
376 over time, assume two situations: low prevalence and high prevalence. When the
377 prevalence is low, the larger pool sizes will result in higher efficiency and lower
378 prevalence (more dilution). However, when the prevalence is high, the 'rescuing'
379 effect will be more prominent and counteract the increasing efficiency and decreasing
380 sensitivity. These results are in line with the widely accepted idea that sample pooling
381 methods show a higher efficiency when pool size is large and that as prevalence
382 increases, it reached a threshold after which smaller pool sizes become more
383 efficient^{1,9}. Intuitively, the 'rescuing' effect is less prominent in 2D pooling strategies,
384 as both pools (row and column) need to rescue the high Cq sample.

385 False negatives have pre-pool Cq values close to the detection limit and
386 predominantly originate from patients who are at the end of an infection^{19,20}, putting

387 their clinical relevance in question (i.e. no longer infectious). Similarly, however, one
388 can argue that these high Cq samples are imperative to a favorable pandemic
389 response: they might originate from pre-symptomatic or very recently-infected
390 patients¹⁹, allowing for catching cases before transmission—a principle at the very
391 core of every population screening strategy. Also, we cannot rule out that these high
392 Cq values are due to imperfect sampling or any other mistakes along the sample
393 preparation¹³.

394 Our study suffers from some essential limitations. First, although the data grouped by
395 weeks provides many different situations to assess, there will still be other
396 combinations of parameters that we did not analyze in this paper. However, the
397 current dataset probably represents the most plausible scenarios as the data
398 originates from a protracted period of the pandemic. Second, we selected only 1D
399 and 2D pooling methods in this simulation study. As stated before, other pooling
400 regimes exist and might be more performant than the discussed ones. Yet, these
401 pooling strategies come with intrinsic shortcomings. The P-BEST pooling protocol is
402 very time consuming¹⁰, even when using a pipetting robot, and the repeated pooling
403 method suffers from a complicated re-pooling scheme¹. Third, our model relies on
404 the critical assumption that we can directly induce the pool's Cq value from the
405 individual samples' Cq values using a simple formula (see Methods). Wet lab
406 experiments have shown that this is not necessarily the case⁵⁻⁸. Fourth, to calculate
407 the pooling strategies' performance, the single-molecule Cq value and the
408 prevalence must be known. However, we can easily calculate the single-molecule Cq
409 value by generating a ddPCR calibrated dilution series as done in this paper. The
410 prevalence, however, cannot be known precisely, and as a result, the prevalence
411 must be estimated. We can do this either before adopting a pooling strategy by

412 testing the individual samples and using the fraction of positive samples as an
413 indication for the prevalence or when a pooling strategy is already in place by
414 calculating it from the percentage of positive pools^{2,19}. Last, the calculated efficiency
415 gain is merely a representation of the number of individual RNA extractions and RT-
416 qPCR reactions and does not evaluate the amount of labor or time-to-result. Pooling
417 a low number of samples will unnecessarily increase the time-to-result and workload.
418 In conclusion, we show that finding the optimal pooling strategy for SARS-CoV-2 test
419 samples is guided by a testing population-dependent efficiency-sensitivity trade-off.
420 Consequently, the most favorable pooling regime might change throughout the
421 pandemic due to epidemiological changes and revisions in diagnostic testing
422 strategies. We provide an accessible shiny application to guide readers towards the
423 optimal pooling strategy to fit their needs.

424

425 **Acknowledgements**

426 We are grateful for the data from the Belgian federal taskforce for COVID-19 qPCR
427 testing.

428

429 Conceptualization: J.Va., P.M. and J.Ve.; Methodology: J.Va., P.M. and J.Ve.;
430 Software: J.Ve., T.S.; Formal Analysis: J.Ve.; Resources: J.H., J.Va. and P.M.; Data
431 Curation: J.Ve.; Writing – Original Draft: J.Va. and J.Ve.; Writing – Review & Editing;
432 J.Va., J.H., P.M., T.S. and J.Ve.; Visualisation: J.Va. and J.Ve.; Supervision: J.Va
433 and P.M.; Project Administration: J.Va. and P.M.

434

435 **Data availability**

436 The code and Cq values are available on

437 <https://github.com/OncoRNALab/covidpooling>.

438 **References**

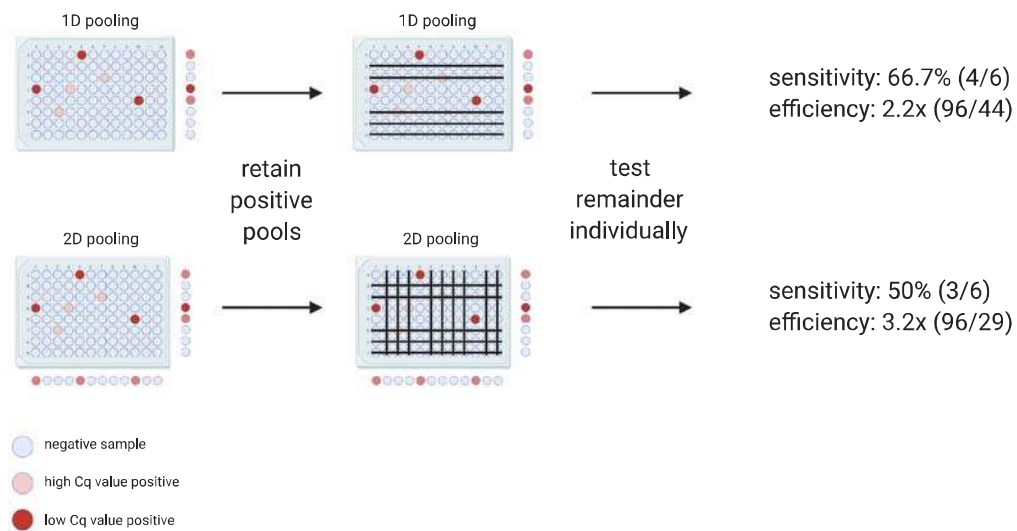
- 439 1. Shani-Narkiss H, Gilday OD, Yayon N, Landau ID. Efficient and Practical
440 Sample Pooling High-Throughput PCR Diagnosis of COVID-19. MedRxiv,
441 2020:2020.04.06.20052159
- 442 2. Guha P, Guha A, Bandyopadhyay T. Application of pooled testing in screening
443 and estimating the prevalence of Covid-19. MedRxiv,
444 2020:2020.05.26.20113696
- 445 3. Adams K. Expanding Covid-19 Testing: Mathematical Guidelines for the
446 Optimal Sample Pool Size Given Positive Test Rate. MedRxiv,
447 2020:2020.05.21.20108522
- 448 4. Milliioni R, Mortarino C. Sequential informed pooling approach to detect SARS-
449 CoV2 infection. MedRxiv, 2020:2020.04.24.20077966
- 450 5. Hogan CA, Sahoo MK, Pinsky BA. Sample Pooling as a Strategy to Detect
451 Community Transmission of SARS-CoV-2. JAMA - J Am Med Assoc, 2020,
452 323:1967–9
- 453 6. Yelin I, Aharony N, Shaer Tamar E, Argoetti A, Messer E, Berenbaum D,
454 Shafran E, Kuzli A, Gandali N, Shkedi O, Hashimshony T, Mandel-Gutfreund
455 Y, Halberthal M, Geffen Y, Szwarcwort-Cohen M, Kishony R, Taub Professor
456 H. Evaluation of COVID-19 RT-qPCR test in multi-sample pools. Clin Infect
457 Dis, 2020. <https://doi.org/https://doi.org/10.1093/cid/ciaa531>
- 458 7. Abdalhamid B, Bilder CR, McCutchen EL, Hinrichs SH, Koepsell SA, Iwen PC.
459 Assessment of Specimen Pooling to Conserve SARS CoV-2 Testing
460 Resources. Am J Clin Pathol, 2020, 153:715–8
- 461 8. Torres I, Albert E, Navarro D. Pooling of nasopharyngeal swab specimens for
462 SARS-CoV-2 detection by RT-PCR. J Med Virol, 2020, 92:2306–7

- 463 9. Sinnott-Armstrong N, Klein D, Hickey B. Evaluation of Group Testing for SARS-
464 CoV-2 RNA. MedRxiv, 2020:2020.03.27.20043968
- 465 10. Shental N, Levy S, Wuvshet V, Skorniakov S, Shalem B, Ottolenghi A,
466 Greenshpan Y, Steinberg R, Edri A, Gillis R, Goldhirsh M, Moscovici K,
467 Sachren S, Friedman LM, Neshet L, Shemer-Avni Y, Porgador A, Hertz T.
468 Efficient high-throughput SARS-CoV-2 testing to detect asymptomatic carriers.
469 Sci Adv, 2020, 6:5961–72
- 470 11. Ghosh S, Agarwal R, Rehan MA, Pathak S, Agrawal P, Gupta Y, Consul S,
471 Gupta N, Goyal R, Rajwade A, Gopalkrishnan M. A Compressed Sensing
472 Approach to Group-testing for COVID-19 Detection. ArXiv, 2020
- 473 12. Gan Y, Du L, Damola FO, Huang J, Xiao G, Lyu X. Sample Pooling as a
474 Strategy of SARS-COV-2 Nucleic Acid Screening Increases the False-negative
475 Rate. MedRxiv, 2020:2020.05.18.20106138
- 476 13. Dahdouh E, Lázaro-Perona F, Romero-Gómez MP, Mingorance J, García-
477 Rodríguez J. Ct values from SARS-CoV-2 diagnostic PCR assays should not
478 be used as direct estimates of viral load. J Infect, 2020.
479 <https://doi.org/10.1016/j.jinf.2020.10.017>
- 480 14. Buchan BW, Hoff JS, Gmehlin CG, Perez A, Faron ML, Munoz-Price LS,
481 Ledebor NA. Distribution of SARS-CoV-2 PCR cycle threshold values provide
482 practical insight into overall and target-Specific sensitivity among symptomatic
483 patients. Am J Clin Pathol, 2020. <https://doi.org/10.1093/AJCP/AQAA133>
- 484 15. Corman VM, Landt O, Kaiser M, Molenkamp R, Meijer A, Chu DK, Bleicker T,
485 Brünink S, Schneider J, Schm ML, Mulders DG, Haagmans BL, van der Veer
486 B, van den Brink S, Wijsman L, Goderski G, Romette J-L, Ellis J, Zambon M,
487 Peiris M, Goossens H, Reusken C, Koopmans MP, Drosten C. Detection of

- 488 2019 novel coronavirus (2019-nCoV) by real-time RT-PCR. *Eurosurveillance*,
489 2020, 25:2000045
- 490 16. Hay JA, Kennedy-Shaffer L, Kanjilal S, Lipsitch M, Mina MJ. Estimating
491 epidemiologic dynamics from single cross-sectional viral load distributions.
492 *MedRxiv*, 2020:2020.10.08.20204222
- 493 17. Singanayagam A, Patel M, Charlett A, Bernal JL, Saliba V, Ellis J, Ladhani S,
494 Zambon M, Gopal R. Duration of infectiousness and correlation with RT-PCR
495 cycle threshold values in cases of COVID-19, England, January to May 2020.
496 *Eurosurveillance*, 2020. [https://doi.org/10.2807/1560-](https://doi.org/10.2807/1560-7917.ES.2020.25.32.2001483)
497 [7917.ES.2020.25.32.2001483](https://doi.org/10.2807/1560-7917.ES.2020.25.32.2001483)
- 498 18. Gorzalski AJ, Hartley P, Laverdure C, Kerwin H, Tillett R, Verma S, Rossetto
499 C, Morzunov S, Hooser S Van, Pandori MW. Characteristics of viral specimens
500 collected from asymptomatic and fatal cases of COVID-19. *J Biomed Res*,
501 2020, 34:431–6
- 502 19. Cleary B, Hay JA, Blumenstiel B, Harden M, Cipicchio M, Bezney J, Simonton
503 B, Hong D, Senghore M, Sesay AK, Gabriel S, Regev A, Mina MJ. Using viral
504 load and epidemic dynamics to optimize pooled testing in resource-constrained
505 settings. *Sci Transl Med*, 2021:eabf1568
- 506 20. Tom MR, Mina MJ. To Interpret the SARS-CoV-2 Test, Consider the Cycle
507 Threshold Value. *Clin Infect Dis*, 2020, 71:2252–4
508
509

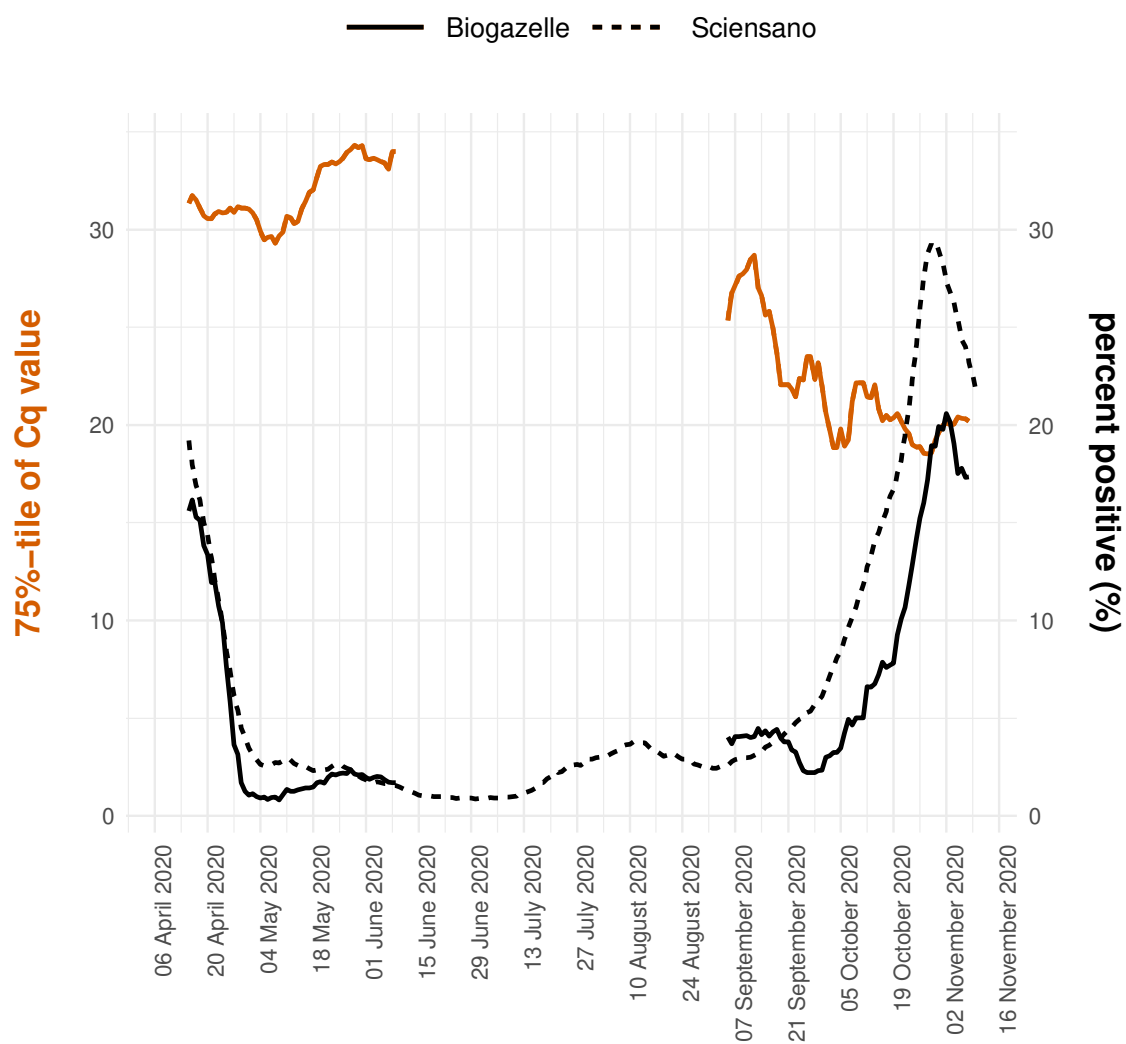
510 **Figures**

511 **Figure 1**



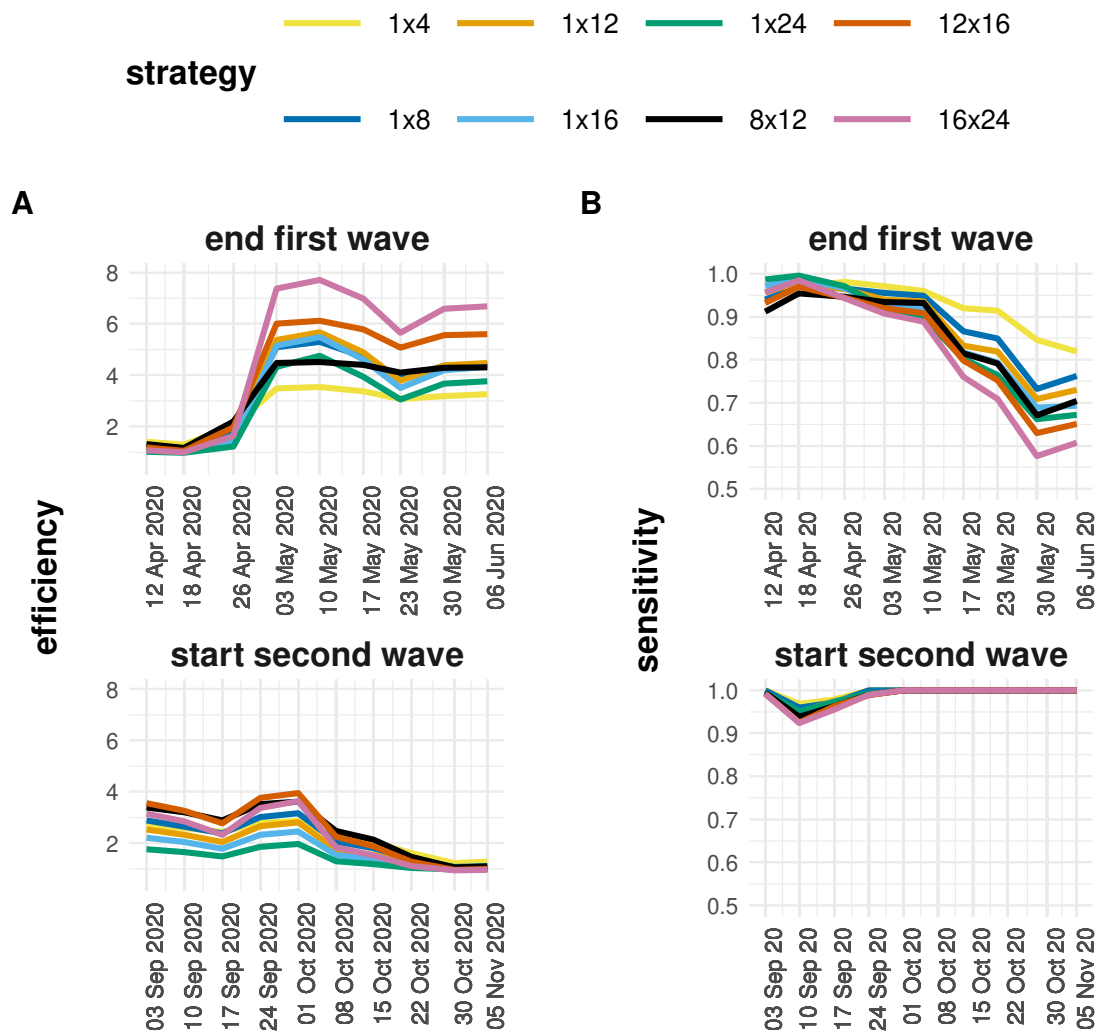
512

513 **Figure 2**



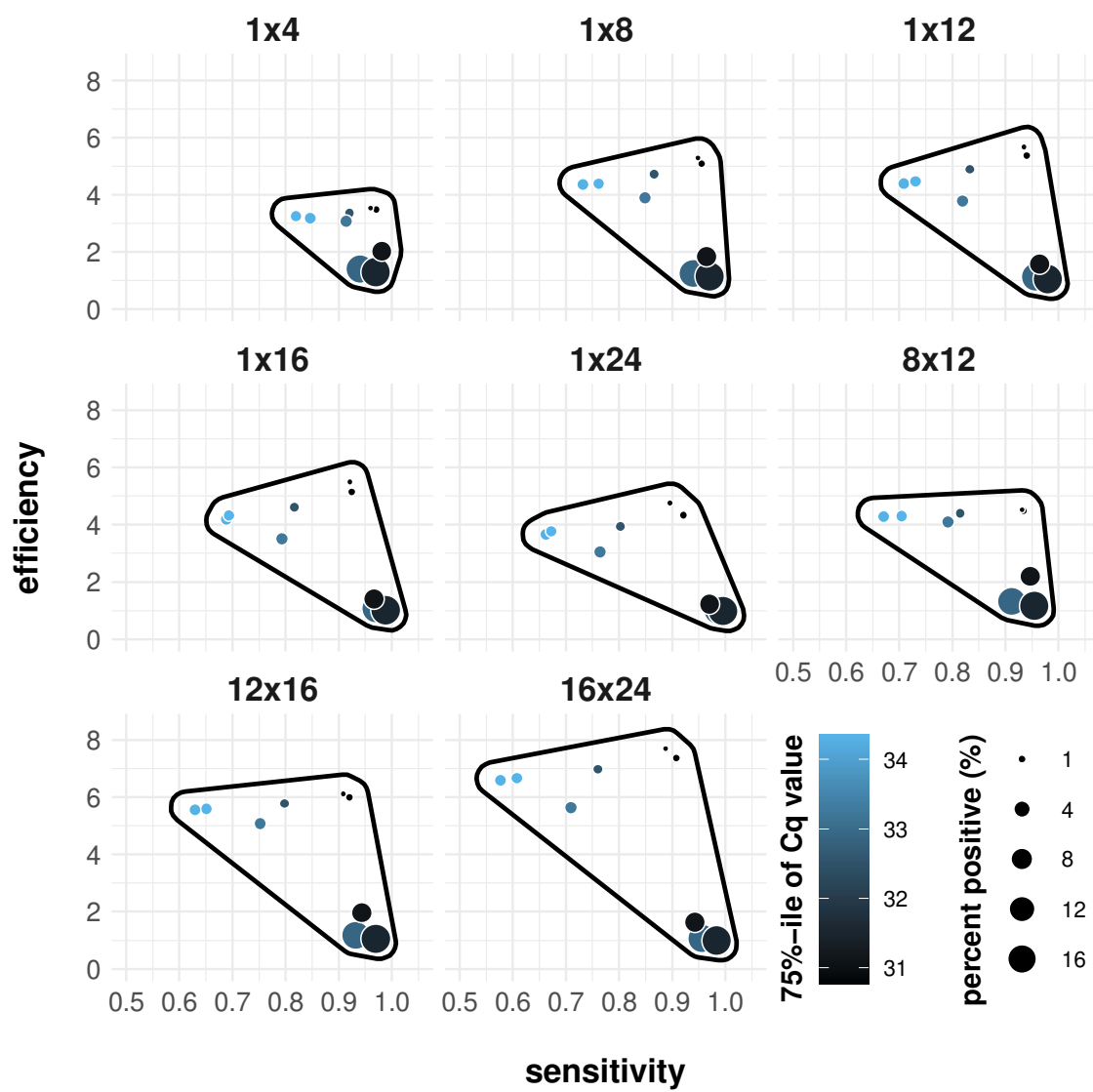
514

515 **Figure 3**



517 **Figure 4**

518



519

520 **Figure Legends**

521 **Figure 1:** Schematic overview of the applied pooling strategies. The samples are represented as wells
522 in a 96-well microtiter plate. The color of the wells indicates the samples' SARS-CoV-2 RNA
523 concentration. In 1D pooling, the pools are created by row, the pools are tested and the samples in
524 positive pools are tested again individually. During 2D pooling, the pools are created by row and
525 column (each sample exists in two pools), the pools are tested, all negative rows and columns are
526 removed and the remaining samples are tested individually. The sensitivity and the efficiency are
527 calculated according to the equations found in the methods.

528 **Figure 2:** Evolution of the 75%-tile of the Cq value distribution and fraction of positive samples. The
529 left y-axis shows the seven day moving window average of the 75%-tile of the Cq value distribution of
530 the data originating from Biogazelle and the right y-axis shows the seven day moving window average
531 of the fraction of positive samples for the Biogazelle and Sciensano data. The two datasets are
532 differentiated by the line type. If the moving average was calculated using on the basis of less than
533 five days (due to no data being available for specific days), the datapoint was removed from the
534 visualization.

535 **Figure 3:** Sensitivity and efficiency for the end of the first (A) and the start of the second (B) Belgian
536 SARS-CoV-2 infection wave. The data is grouped by week and the sensitivity and efficiency are
537 calculated by simulating different pooling strategies (1x4, 1x8, 1x12, 1x16, 1x24, 8x12, 12x16 and
538 16x24). The pooling strategies can be distinguished by color.

539 **Figure 4:** Simulated sensitivity and efficiency for the end of the first wave visualized with relation to
540 the week (different circles), fraction of positive samples (size of circles) and 75%-tile of the Cq value
541 distribution (color). A polygon is drawn around the datapoints (with a small margin) to visualize and to
542 compare the variability of the sensitivity and efficiency over a period of time between pooling
543 strategies.

544

545

546

547

548

549

550

551 **Supplemental Information to *Evaluation of efficiency and sensitivity***

552 ***of 1D and 2D sample pooling strategies for SARS-CoV-2 RT-qPCR***

553 ***screening purposes***

554

555 **Jasper Verwilt^{1,2,3}, Jan Hellemans⁴, Tom Sante^{2,3}, Pieter Mestdagh^{1,2,3,4}, Jo**

556 **Vandesompele^{1,2,3,4}**

557 *1 OncoRNALab, Cancer Research Institute Ghent, Corneel Heymanslaan 10, 9000*

558 *Ghent, Belgium*

559 *2 Department of Biomolecular Medicine, Ghent University, Corneel Heymanslaan 10,*

560 *9000 Ghent, Belgium*

561 *3 Center for Medical Genetics, Ghent University, Corneel Heymanslaan 10, 9000*

562 *Ghent, Belgium*

563 *4 Biogazelle, Technologiepark-Zwijnaarde 82, 9052 Gent, Belgium*

564

565

566

567 • 4 supplemental figures

568

569

570

571

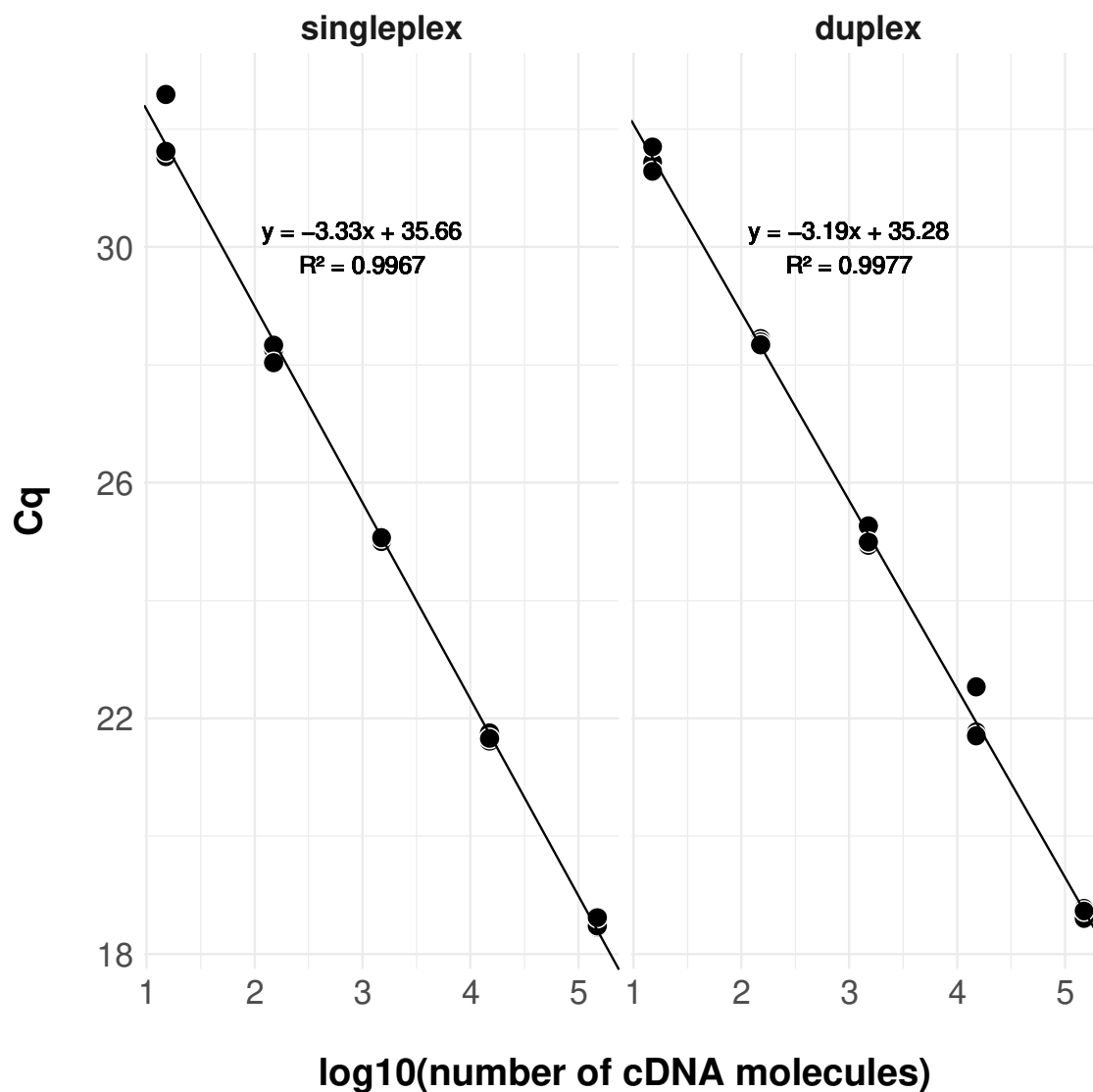
572

573

574

575 **Supplemental Figures**

576

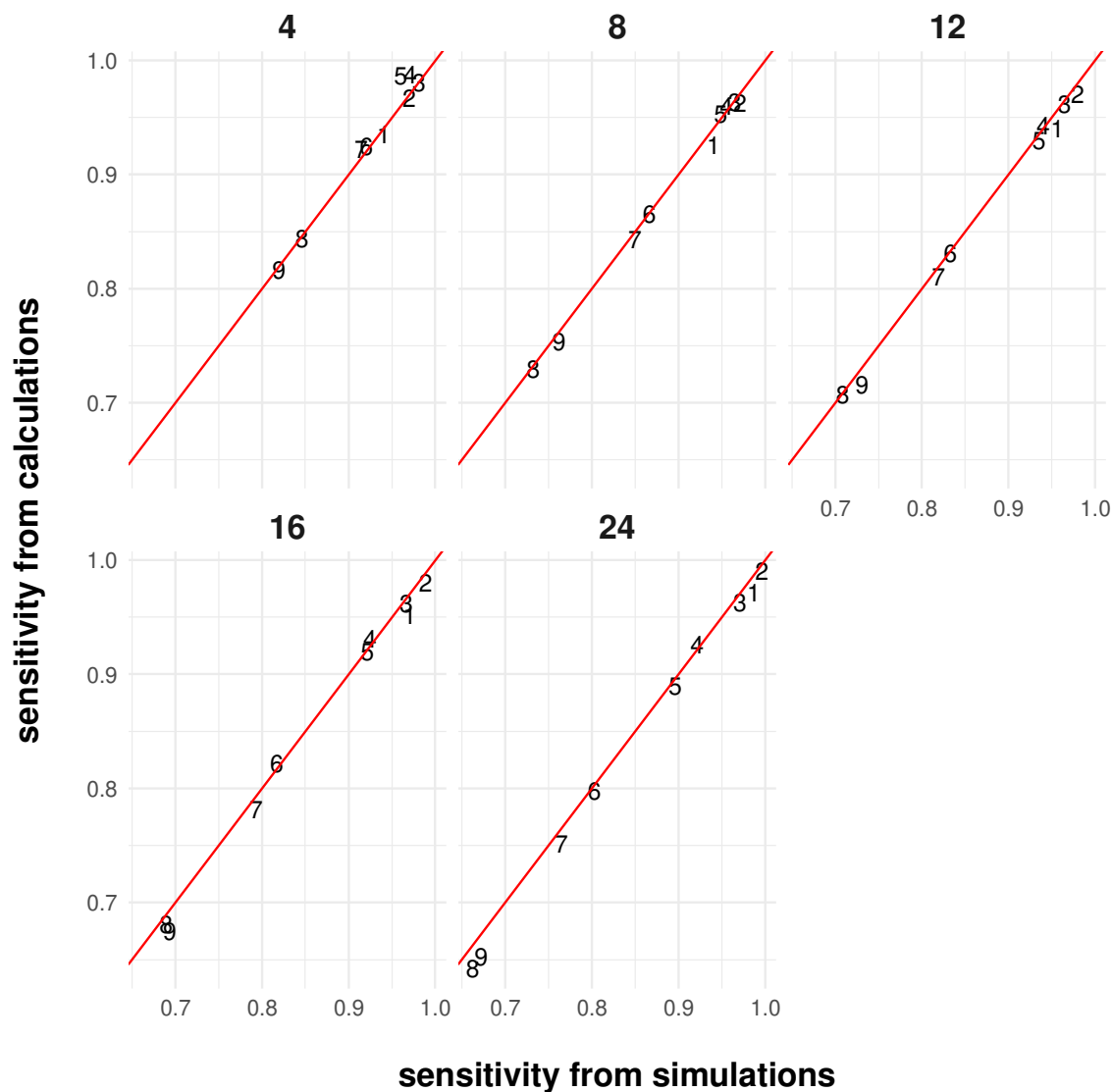


577

578 **Supplemental Figure 1:** Sensitivity analysis of singleplex and duplex qPCR assays using
579 predetermined number of cDNA molecules. R-squared values are adjusted using the Wherry formula.

580 Each number of cDNA molecules was tested in triplicate.

581



582

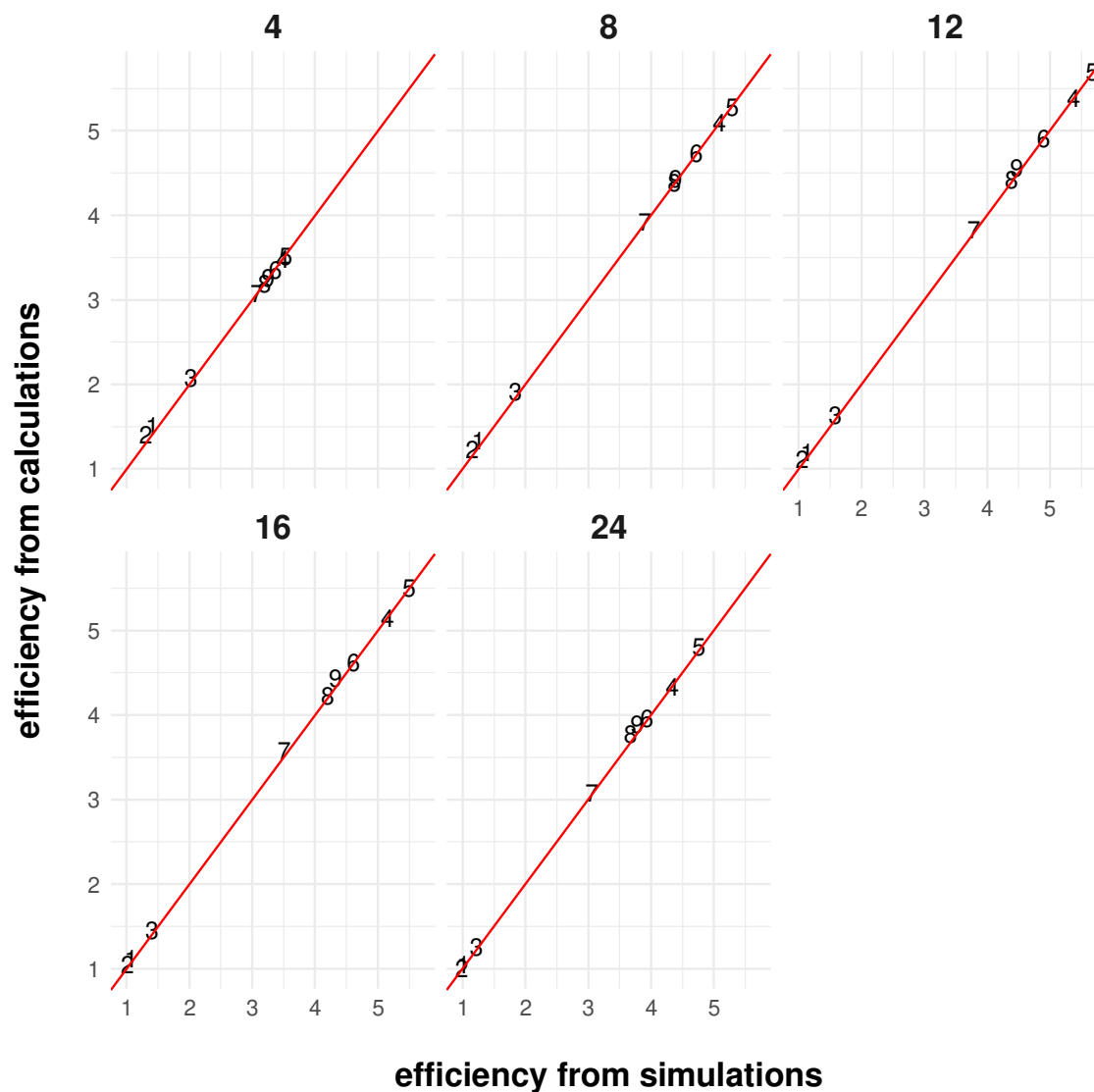
583 **Supplemental Figure 2:** Concordance of sensitivity estimations between simulations and calculations

584 for the end of the first Belgian SARS-CoV-2 infection wave. The numbers represent the weeks (1: 1st

585 week; 2: 2nd week; ...) and are plotted at the sensitivities derived from the simulations and

586 calculations. The red line represents the points where both values are equal.

587



588

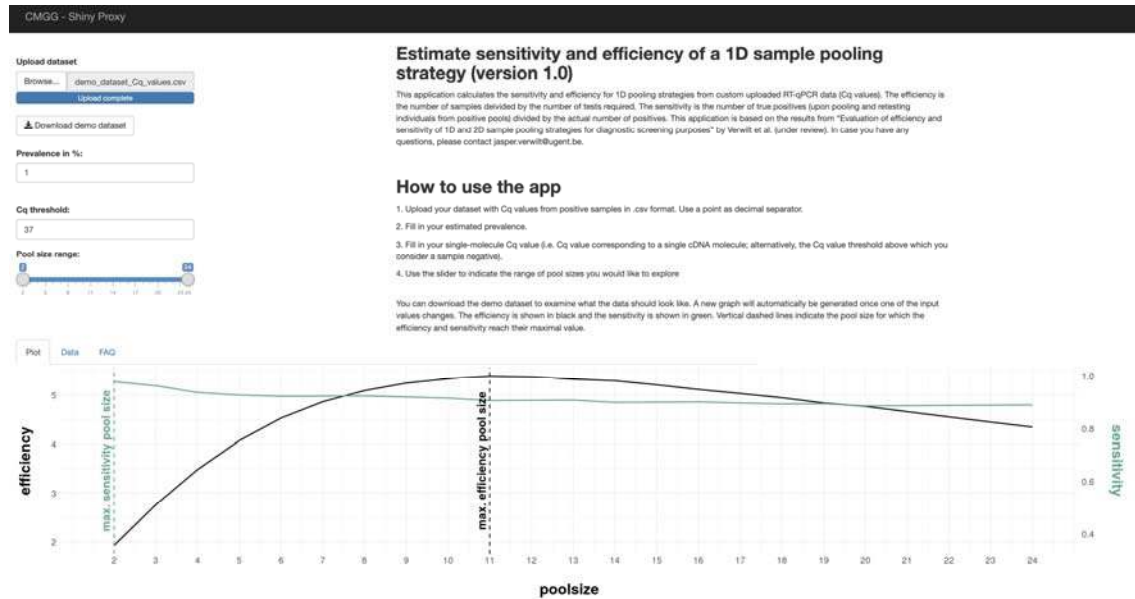
589 **Supplemental Figure 3:** Concordance of efficiency estimations between simulations and calculations

590 for the end of the first Belgian SARS-CoV-2 infection wave. The numbers represent the weeks (1: 1st

591 week; 2: 2nd week; ...) and are plotted at the efficiencies derived from the simulations and calculations.

592 The red line represents the points where both values are equal.

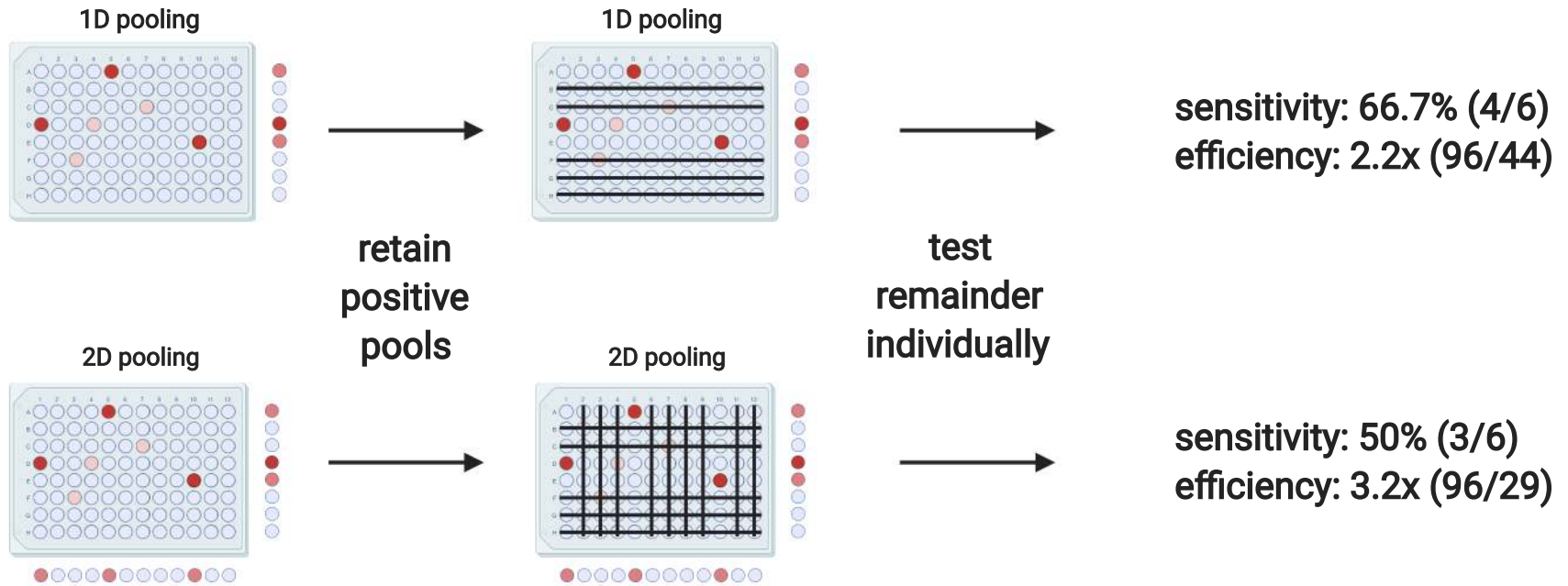
593



594

595 **Supplemental Figure 4:** A screenshot of the interface of the Shiny application. The webpage
596 provides the user with a short description and a detailed outline of how to use the application. In the
597 upper left corner, the user can provide their dataset. If the user would prefer to first explore the app
598 without using their own data, a demo dataset can be downloaded and used instead. The user can fill
599 in the estimated prevalence and single-molecule Cq value. The slider underneath can be used to
600 indicated which range of pool sizes the user wishes to explore. Upon uploading the data, a graph will
601 be outputted in the "Plot" tab, showing the estimated sensitivity and efficiency of each pool size. The
602 vertical dashed lines represent the pool size at which the corresponding parameter reaches its
603 maximal value for this data. The "Data" tab provides the user with a tabulated overview of the
604 estimated sensitivity and efficiency of each pool size.

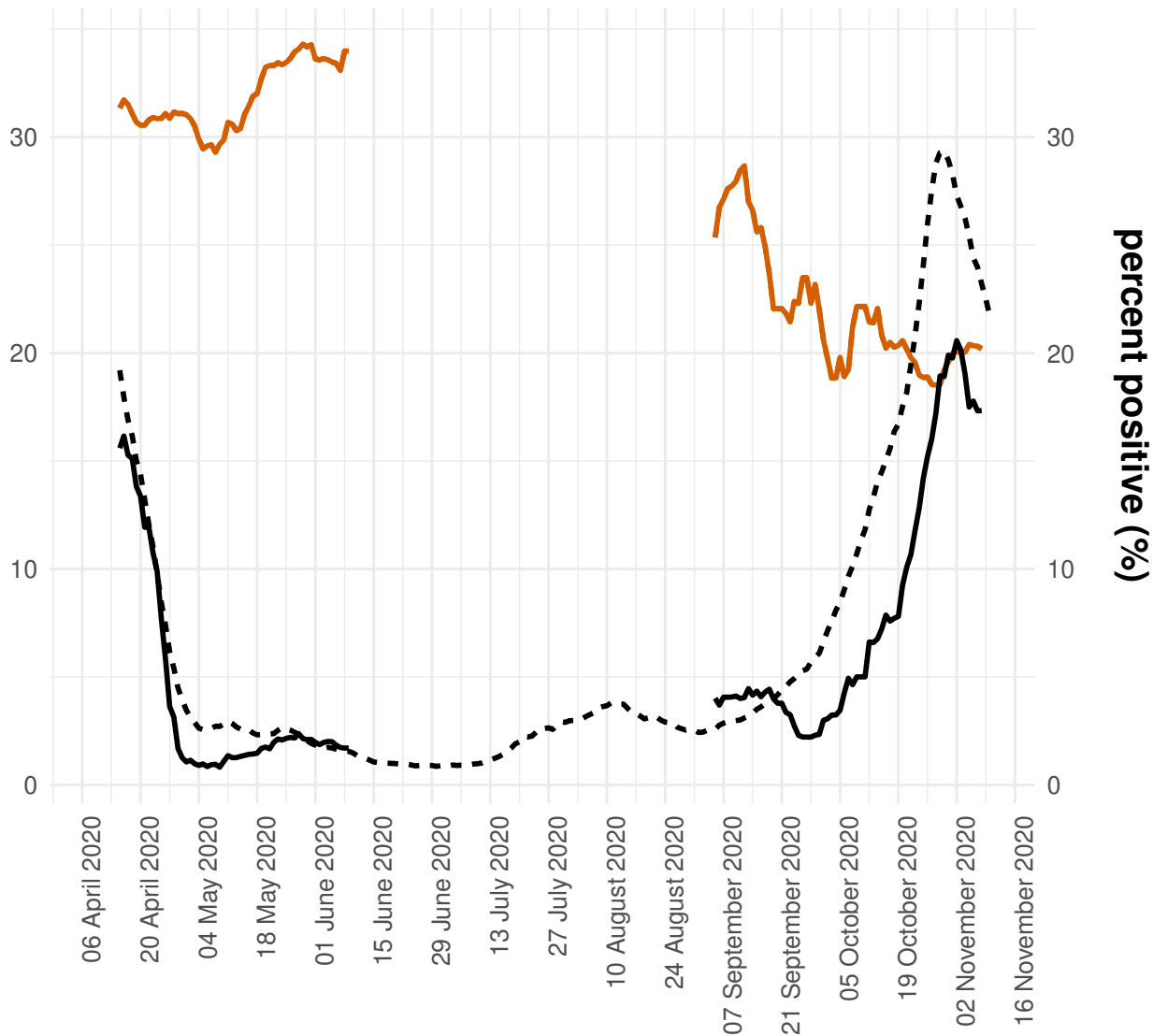
605



- negative sample
- high Cq value positive
- low Cq value positive

75%--tile of Cq value

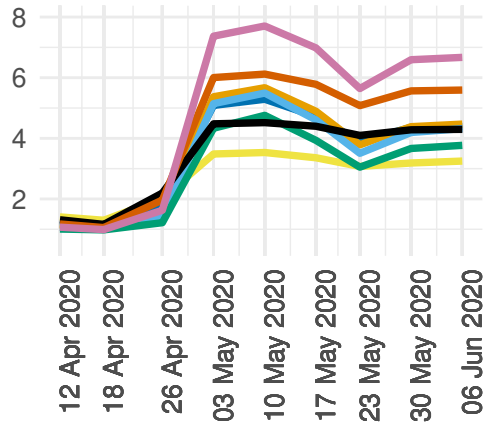
— Biogazelle - - - Sciensano



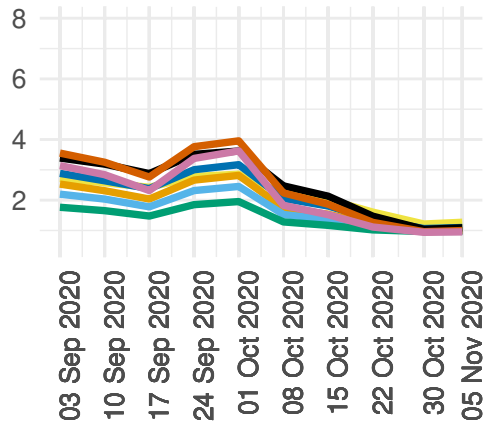


A

end first wave

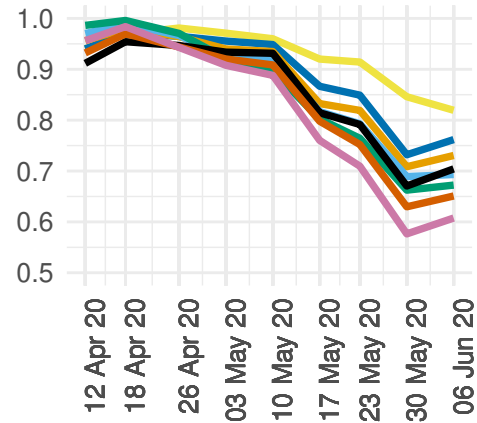


start second wave

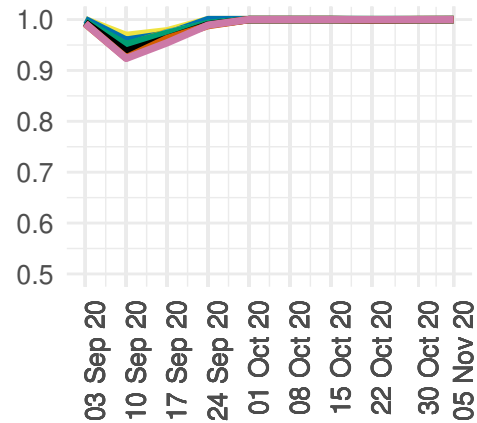


B

end first wave

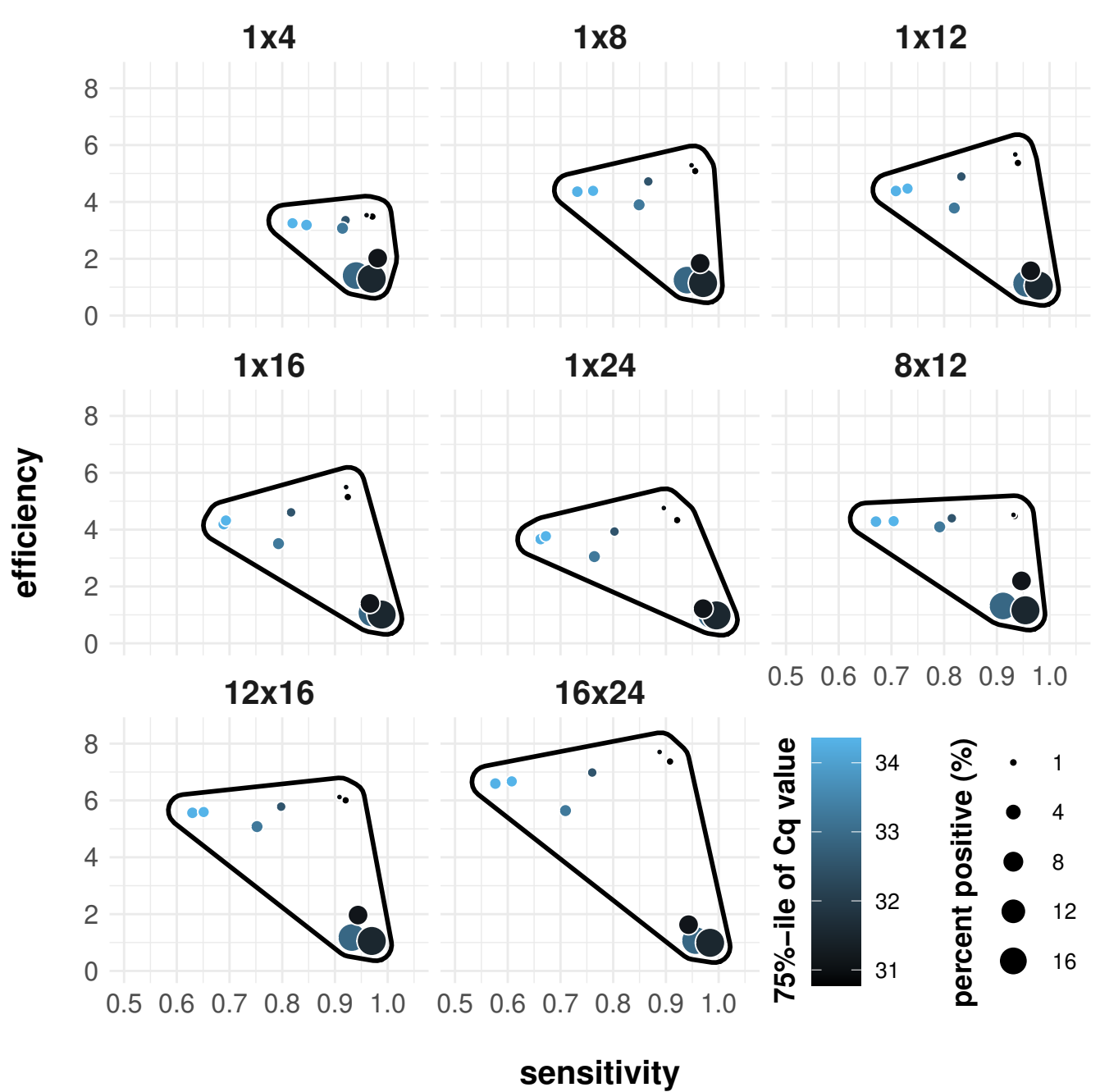


start second wave



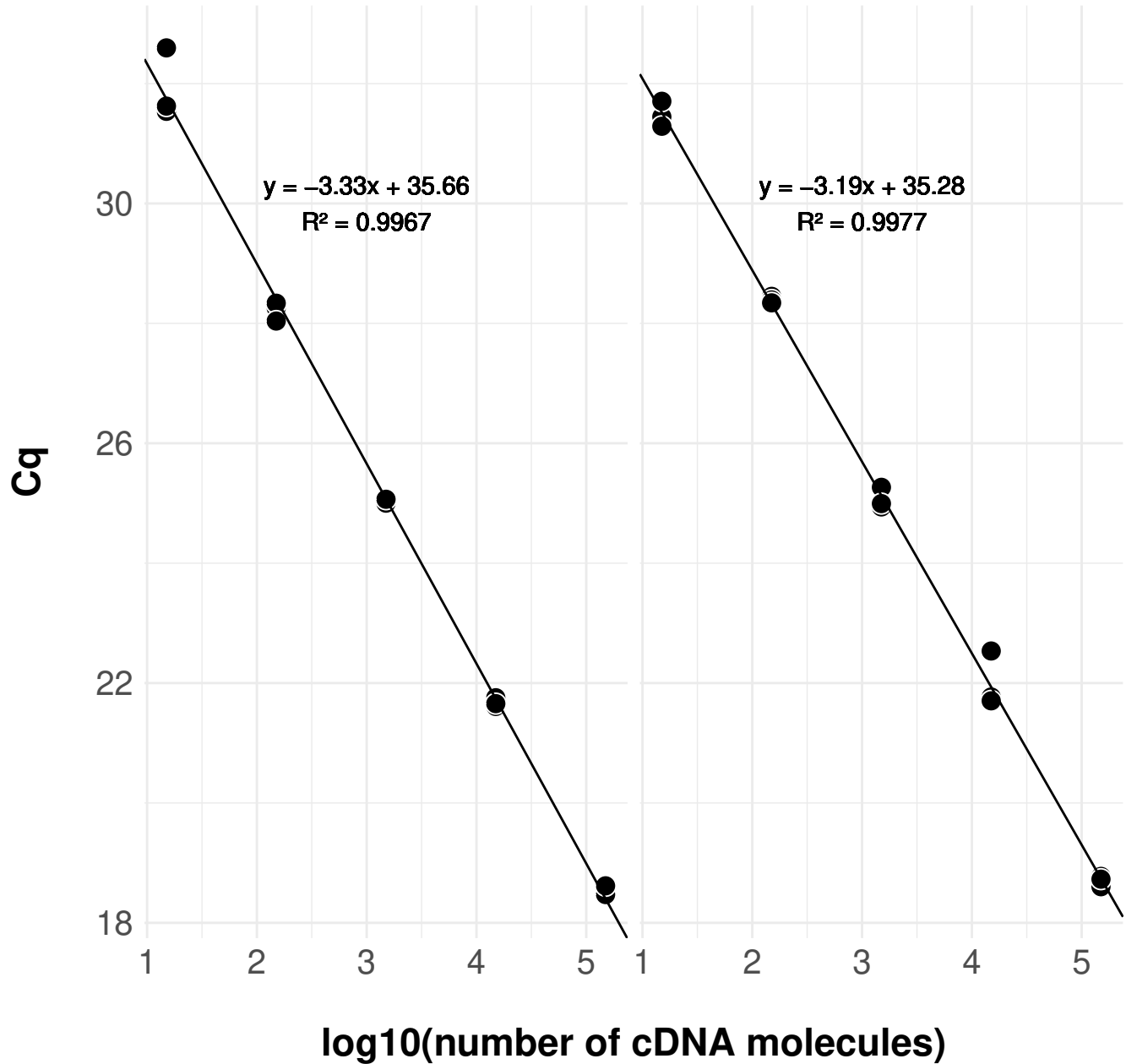
efficiency

sensitivity



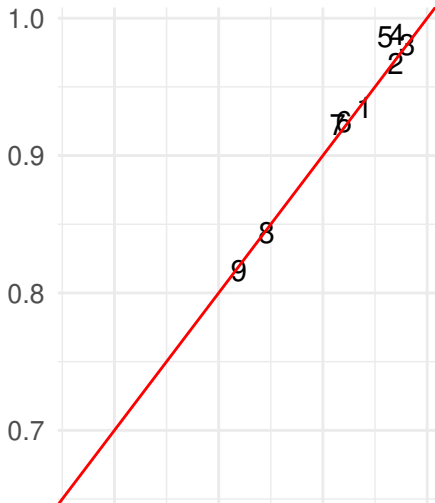
singleplex

duplex

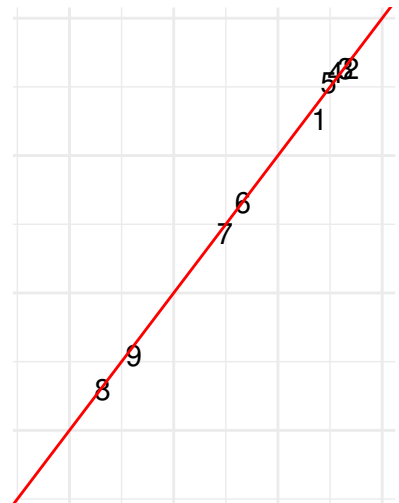


sensitivity from calculations

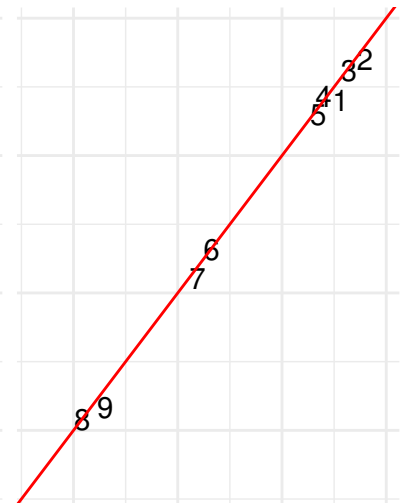
4



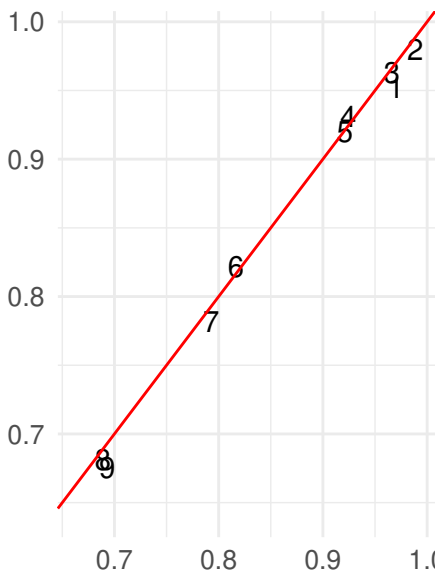
8



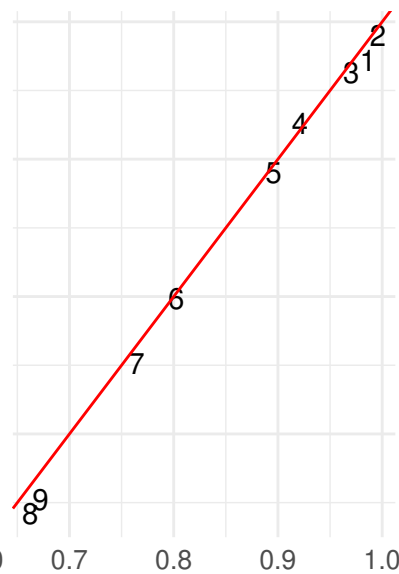
12



16



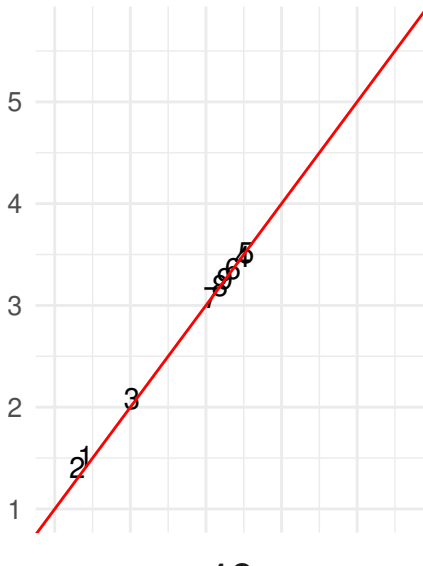
24



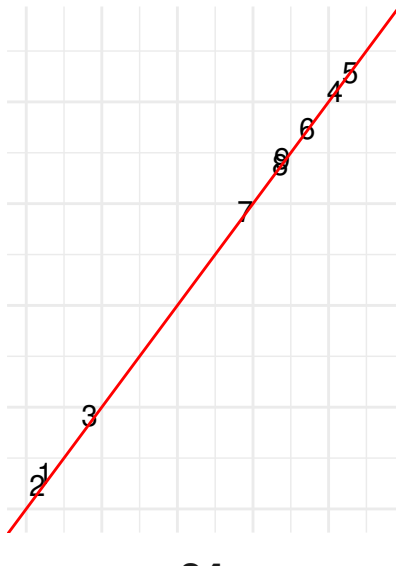
sensitivity from simulations

efficiency from calculations

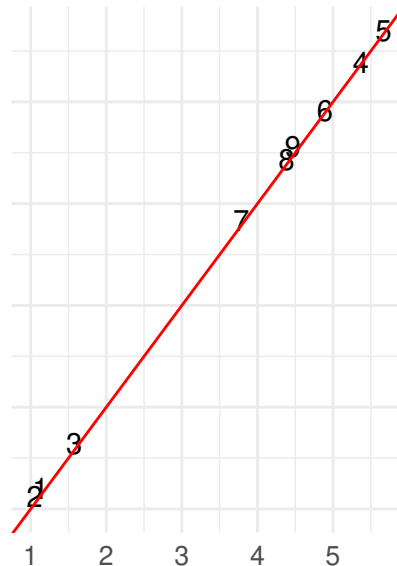
4



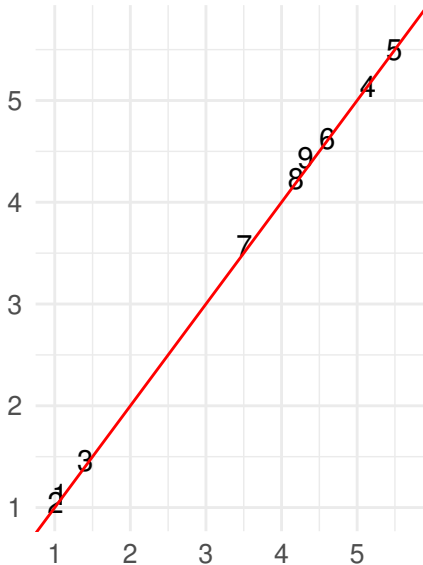
8



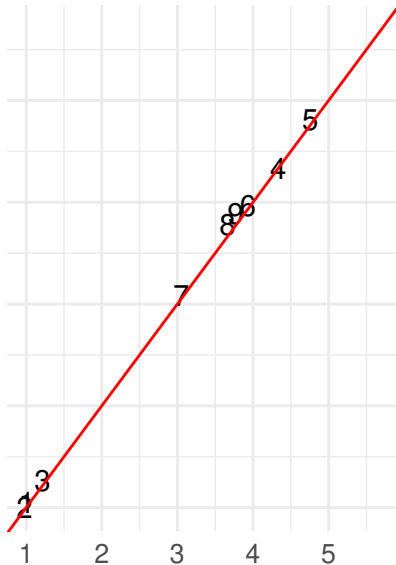
12



16



24



efficiency from simulations

Estimate sensitivity and efficiency of a 1D sample pooling strategy (version 1.0)

This application calculates the sensitivity and efficiency for 1D pooling strategies from custom uploaded RT-qPCR data (Cq values). The efficiency is the number of samples divided by the number of tests required. The sensitivity is the number of true positives (upon pooling and retesting individuals from positive pools) divided by the actual number of positives. This application is based on the results from "Evaluation of efficiency and sensitivity of 1D and 2D sample pooling strategies for diagnostic screening purposes" by Verwilt et al. (under review). In case you have any questions, please contact jasper.verwilt@ugent.be.

How to use the app

1. Upload your dataset with Cq values from positive samples in .csv format. Use a point as decimal separator.
2. Fill in your estimated prevalence.
3. Fill in your single-molecule Cq value (i.e. Cq value corresponding to a single cDNA molecule; alternatively, the Cq value threshold above which you consider a sample negative).
4. Use the slider to indicate the range of pool sizes you would like to explore

You can download the demo dataset to examine what the data should look like. A new graph will automatically be generated once one of the input values changes. The efficiency is shown in black and the sensitivity is shown in green. Vertical dashed lines indicate the pool size for which the efficiency and sensitivity reach their maximal value.

Upload dataset

Browse... demo_dataset_Cq_values.csv

Upload complete

Download demo dataset

Prevalence in %:

1

Cq threshold:

37

Pool size range:

2

24

2 5 8 11 14 17 20 23 24

medRxiv preprint doi: <https://doi.org/10.1101/2020.07.17.20152702>; this version posted April 15, 2021. The copyright holder for this preprint (which was not certified by peer review) is the author/funder, who has granted medRxiv a license to display the preprint in perpetuity. It is made available under a [CC-BY-NC 4.0 International license](https://creativecommons.org/licenses/by-nc/4.0/).

Plot

Data

FAQ

